Available online at www.sciencedirect.com

ScienceDirect

Procedia CIRP 144 (2026) 411–416

www.elsevier.com/locate/procedia

8th CIRP Conference on Surface Integrity

Utilizing intermediate feature value correlation for efficient parameter identification in high-speed directed energy deposition

Helena Wexel[a]*, Keisuke Nagato[b], Frederik Zanger[a]

[a]wbk Institute of Production Science, Karlsruhe Institute of Technology, Kaiserstr. 12, 76131 Karlsruhe, Germany
[b]Department of Mechanical Engineering, Graduate School of Engineering, The University of Tokyo, Japan

* Corresponding author. Tel.: +49 721 608 44288; *E-mail address:* helena.wexel@kit.edu

Abstract

Powder-based high-speed directed energy deposition with laser beam (HS DED-LB) is a key enabler for circular and resource-efficient manufacturing, combining high deposition velocities up to 200 m/min and layer heights down to 50 µm. However, determining suitable process parameters based on conventional ex-situ analyses remains time-consuming and cost-intensive. This explorative study employs an in-between extraction method to determine intermediate feature values of two-layer samples. To characterize the properties of the two-layer samples surface texture measurements and hardness measurements were performed. The feature values were then correlated with key quality metrics, specifically porosity and hardness. The findings demonstrate that surface texture parameters, when used as intermediate feature values, can serve as indicators of the final component density, enabling faster and more cost-efficient process parameter identification. In particular, the correlation between surface-level feature data and subsurface defects highlights the potential of surface-based monitoring as an effective means of assessing component quality. This contributes to more reliable and functionally robust components in high-performance applications and broadens the applicability of HS DED-LB in circular production environments.

© 2026 The Authors. Published by Elsevier B.V.
This is an open access article under the CC BY-NC-ND license (https://creativecommons.org/licenses/by-nc-nd/4.0)
Peer-review under responsibility of the scientific committee of the Scientific committee of the CIRP CSI 2026

Keywords: High-Speed Directed Energy Deposition; Additive Manufacturing; Intermediate Feature Value; Porosity; Hardness

1. Introduction

The increasing demands for sustainable and circular production have made the extension of component lifetimes through remanufacturing a strategic priority. Remanufacturing is a standardized, value-retaining process in which products with at least the original functionality are created from reprocessed components, often combining subtractive and additive operations to maximize value retention [1]. Moreover, remanufacturing enhances resource efficiency and supports circular economy principles across industries [2, 3].

Within these approaches, additive manufacturing (AM), particularly powder-based directed energy deposition using a laser beam (DED-LB), plays a central role. DED-LB enables the production and reprocessing of near-net-shape components by successive material addition and is a key metal-based AM technology alongside powder bed fusion (PBF-LB) [4]. Its ability to integrate multiple materials within a single component, produce multifunctional structures, and deposit material on complex surfaces using 5-axis systems makes it highly versatile for reprocessing applications.

A particularly advanced variant is high-speed directed energy deposition with laser beam (HS DED-LB), also referred to as EHLA (Extremes Hochgeschwindigkeits-Laserauftrag-schweißen). Unlike conventional DED-LB, HS DED-LB focuses the powder stream above the substrate, preheating and partially or fully melting the particles before they reach the melt pool. This enables processing speeds of up to 200 m/min with significantly reduced heat input, resulting in smaller melt pools, narrower heat-affected zones, and shorter processing times [5, 6]. Powder mass flow rate, processing speed, and laser power exert the strongest influence on the process [7]. Furthermore,

2212-8271 © 2026 The Authors. Published by Elsevier B.V.
This is an open access article under the CC BY-NC-ND license (https://creativecommons.org/licenses/by-nc-nd/4.0)
Peer-review under responsibility of the scientific committee of the Scientific committee of the CIRP CSI 2026
10.1016/j.procir.2026.02.004

the precise control of powder–laser and powder–laser–substrate interaction times offers the potential to tailor mechanical properties, such as hardness and strength. These characteristics make HS DED-LB particularly promising for reprocessing and surface functionalization.

However, efficient process parameter identification remains a major challenge. Especially, since the component geometry affects heat dissipation and requires parameter adjustment [8]. Relative density, which reflects the ratio of material to pores in the manufactured structure [6], is widely used as an indicator of material quality and process performance. However, its determination typically relies on time-consuming experimental analysis of bulk samples, e.g. with computer tomography (CT) measurements or metallographic cross-sections. This limitation is particularly restrictive in the context of remanufacturing, where parameter studies must often be conducted across a wide range of materials. Recent studies have highlighted the potential of using intermediate feature values (IFV) as predictive indicators of final material properties [9, 10]. Such features can serve as proxies for mechanical characteristics, enabling faster and more cost-efficient identification of suitable process parameters. This approach holds particular promise for HS DED-LB, where the interplay between process parameters, material properties, and resulting component quality is complex and requires efficient evaluation methods. Therefore, this work investigates an explorative approach for efficient process parameter identification in HS DED-LB, using surface texture parameters from two-layer samples as IFV to predict the density and hardness of bulk samples.

2. State of the Art

The outcome of directed energy deposition processes is strongly dependent on several process control variables [11]. According to Greco et al., the variables of laser power, powder mass flow, and processing speed, as well as their interrelationships, have a decisive influence on the resulting mechanical properties of the component [7]. Schaible et al. further demonstrated that targeted adjustment of these parameters substantially affects process outcomes [12].

An experimental approach to identify relevant process parameters and their appropriate ratios was described by Sciammarella et al. for conventional DED of 316L stainless steel [13]. Platz et al. performed a parameter study on HS DED-LB, varying laser power and processing speed for different numbers of 17-4 PH layers, and subsequently analyzed the resulting microhardness and density via microsections [14]. In addition, Schopphoven investigated process relevant influencing factors such as transmittance, particle heating in the beam path and heating of the substrate [3]. These studies collectively highlight the complexity of the process and underline that the identification of a stable and sufficient process window for different materials in HS DED-LB remains an extensive and resource-intensive task.

In parallel, recent research has shown that IFV can serve as predictive indicators of final material properties [9, 10]. Nagato et al. proposed an approach to efficiently determine density and pore size in porous PBF-LB-manufactured samples. IFV were extracted from surface profiles obtained by confocal laser microscopy and compared with intermediate feature values derived from binary optical microscopy images. While pore size could be predicted with sufficient accuracy, the prediction of density was found to be limited [10]. Other studies have demonstrated the use of in-situ process observations as a source of IFV. For example, [9] proposed analyzing spatter particles captured by high-speed imaging, reasoning that the amount of spatter must reflect the physical phenomena of the PBF. Regression analysis revealed that incorporating the amount of spatter into the prediction model significantly improved accuracy. In particular, the coefficient of determination R^2 for Vickers hardness prediction increased from 0.17, using only volumetric energy density, to 0.54 when spatter information was added. Similarly, for density prediction, R^2 improved from 0.31 to 0.58. [9] However, the implementation of high-speed imaging requires extensive expertise and substantial financial investment, which limits its industrial applicability.

Although IFV-based approaches are well established in additive manufacturing, their transfer to HS DED-LB, with its high processing speeds and distinct powder–laser interactions, remains limited. Therefore, this study aims to transfer the IFV concept to HS DED-LB. Additionally, this study explores the use of surface texture parameters - surface S, roughness R, waviness W, primary profile P - from confocal microscopy analysis as a more straightforward and cost-efficient method to extract IFV. Unlike time-consuming and destructive ex-situ analyses such as CT or metallography, surface texture measurements can be performed rapidly on early layers of the build. It is hypothesized that surface texture parameters also reflect the physical phenomena of the HS DED-LB process, containing information of track geometry, homogeneity and spatter. This approach aims to avoid the need for additional, complex equipment while still enabling reliable prediction of key quality metrics such as density.

3. Materials and Methods

The present study used AISI 4140 (42CrMo4) powder from m4p material solutions GmbH with a particle size ranging from 20 µm to 53 µm deposited on substrates of the same material.

The powder was additionally analyzed by dynamic image analysis using a Camsizer X2 from Microtrac Retsch GmbH with regard to particle size distribution (PSD) and shape parameters. $D_{10} = 25.1$ µm, $D_{50} = 35$ µm, $D_{90} = 47.9$ µm and the SPAN value with SPAN = 0.652 µm were determined.

All experiments were conducted on a pE3D HS DED-LB system of Ponticon GmbH. A powder feeder (BLC Lasercladding GmbH PF2-2 MFR) and a high power diode laser (Laserline GmbH LDF 6000-40) were used in conjunction with a coaxial powder nozzle (Laserline GmbH RP13). A PowderSpy (Ponticon GmbH) was used to optically examine the powder-gas stream and set the powder focus 1 mm above the substrate. Samples were produced with a 0.5 mm hatch distance, a laser spot diameter of $d_L = 1$ mm and a powder mass flow rate of $\dot{m} = 15$ g/min, using a bidirectional scanning strategy rotated 67° per layer. The argon carrier gas flow rate $\dot{V}_{cg}$ was 8 l/min, the argon shielding gas flow rate was $\dot{V}_{sg} = 20$ l/min. To investigate the influence of key process parameters on the HS DED-LB process, the laser power P_L was varied between 2350 W and 2650 W in $\Delta P_L = 75$ W steps and the processing speed v was varied between 40 m/min and 60 m/min in $\Delta v = 5$ m/min steps, according to Figure 1.

P_L in W \ v in m/min	40	45	50	55	60
2350	x		x		x
2425		x	x	x	
2500	x	x	x	x	x
2575		x	x	x	
2650	x		x		x

Fig. 1. Variations of laser power and processing speed, printed parameter combinations marked by x.

Two-layer samples with an area of 20×20 mm^2 as well as 10 mm*10 mm*3 mm bulk samples were manufactured. As illustrated in Figure 2. surface analysis of the two-layer samples was performed using a LEXT OLS4500, EVIDENT Co., Ltd. confocal microscope, considering both areal and profile-based texture parameters perpendicular to the top scan direction, with three measurement points per parameter combination.

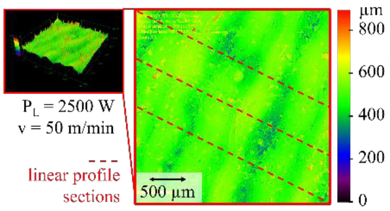

Fig. 2. Representative procedure for confocal laser microscope measurement.

The density was determined by optical density analysis of the bulk samples using a Keyence VHX-8000 digital microscope, with three areas measured per sample perpendicular to the build direction. The Vickers hardness HV1 of the bulk samples was measured using a Shimadzu HMV-G21st at three points each on the sample top and bottom, following DIN EN ISO 6507. The line energy density $E_L = P_L/v$ is a frequently employed value to evaluate the outcomes of (HS) DED-LB processes [15, 16]. Consequently, density and hardness results were initially analyzed in relation to E_L.

To evaluate the predictive capability of process and surface texture parameters with respect to density and hardness, a Partial Least Squares (PLS) regression in JMP 18 was used. PLS was selected due to the small sample size (n = 17) in combination with a large number of potentially correlated explanatory variables, which makes conventional regression methods such as ordinary least squares prone to overfitting [17]. Two models were investigated: a baseline model considering only the primary process parameters (P_L, v, E_L) and an extended model including surface texture parameters as intermediate features. For the latter, both areal and profile-based surface texture metrics were determined, and the variables contributing most to the response were selected based on the Variable Importance in Projection (VIP) criterion. For this the number of latent factors was fixed to two for the density model and to three for the hardness model, based on minimum Root Mean PRESS and the van der Voet significance test. A threshold of VIP > 1 was applied to ensure that only variables with strong predictive relevance were retained. All PLS analyses were performed using the SIMPLS algorithm. Model validation was carried out by 5-fold cross-validation, with the number of latent factors varied up to ten. Each model was repeated 20 times for cross-validation and R^2, the predictive relevance Q^2 and the van der Voet T^2 statistic were evaluated to assess model fit and predictive stability.

4. Results

4.1. Density analysis

Although all samples exhibit high relative density (>99.4%), the parameter variations produce a range of pore sizes and types, as shown in Figure 3. It can be concluded that within the selected parameter range, different defect mechanisms, e.g. lack of fusion due to insufficient energy input, or the formation of spherical gas pores due to excessive energy input, are present. The size and shape of the defects play a significant role in influencing the material properties [18].

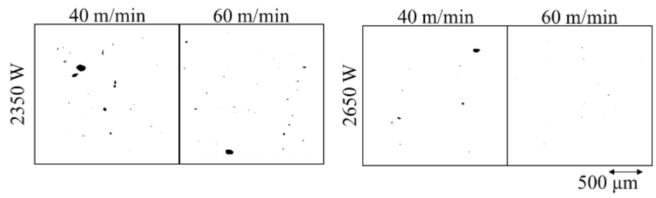

Fig. 3. Exemplary binary images of microsections to assess relative density.

The means and standard deviations of the optical density analysis for the bulk samples are shown in Figure 4. There is no clear correlation to linear energy or laser power.

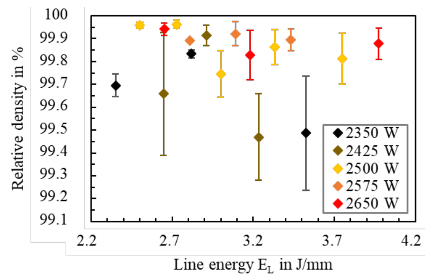

Fig. 4. Relative density for every parameter combination, comparing different laser powers.

4.2. Hardness analysis

Figure 5 displays the mean values and standard deviations of the Vickers microhardness. The values obtained in this study exceed those of conventionally manufactured AISI 4140 and are comparable to those of samples manufactured with PBF-LB [19]. The results obtained from the lower measuring points at the base of the samples are compared with the upper measuring points. With the exception of parameter combinations 1, 2, and 14, the hardness values of the lower measuring points are marginally higher than those of the upper measuring points. The mean discrepancy was found to be 2.7%, with a maximum disparity of 7.4%. As the number of deposited layers increases, the accumulated heat in the deposited region promotes further nucleation growth, resulting in reduced hardness in the upper sections of the bulk samples [20]. No discernible correlation between microhardness and linear energy or laser power is apparent. For the subsequent regression analysis, the hardness values of the lower measuring points are employed.

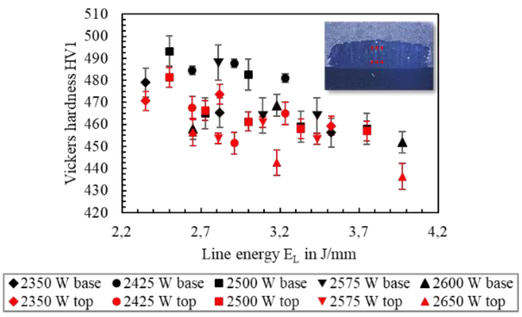

Fig. 5. Vickers microhardness for every parameter combination, comparing measurements at the base and top of the samples.

4.3. Regression analysis

PLS regression models were developed to predict density and hardness. For each target variable, baseline models including only process parameters (P_L, v, E_L) were compared with extended models incorporating surface texture parameters selected via VIP > 1. In Figure 6 the VIP selected for the density and hardness model are depicted.

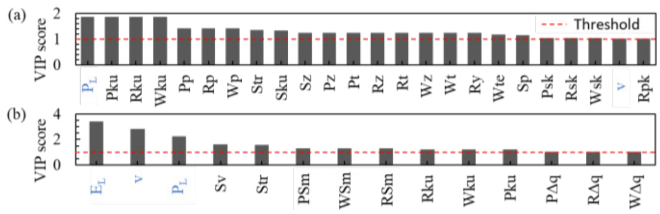

Fig. 6. Selected VIP for (a) density model; (b) hardness model. Process related parameters (P_L, v, E_L) are highlighted in blue.

For density, the baseline model including only process parameters showed very limited predictive ability, with consistently negative Q^2 values. With two latent factors the only Root Mean PRESS < 1 and a cumulative $R^2 \approx 0.44$ was achieved. This confirms that process parameters alone are insufficient to describe the occurrence of pores.

In contrast, the extended model incorporating surface texture parameters as intermediate feature values substantially improved model quality. With three latent factors the mean prediction error is minimized (Root Mean PRESS ≈ 0.77). The extended model reached a mean cumulative $Q^2 \approx 0.59$ and mean cumulative $R^2 \approx 0.85$. These results demonstrate that the addition of surface texture parameters as intermediate feature values capture essential variance related to porosity formation and allow for a more robust prediction. To visualize the improvement, a predicted versus actual value plot for a representative model run, including deviation bands of ±0.1% relative to the ideal line, is shown in Figure 7.

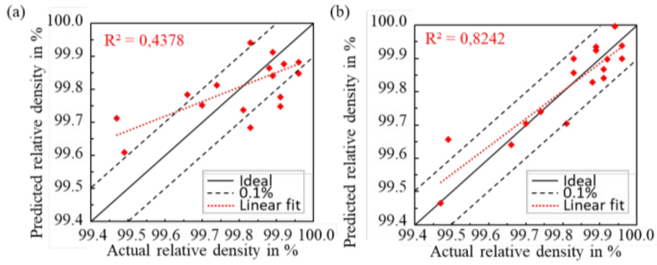

Fig. 7. Results of representative PLS regression models for relative density prediction: predicted versus actual values with deviation bands of ±0.1 % relative to the ideal line for (a) baseline model and (b) extended model.

For hardness, the baseline models already provided a reasonable fit. With one latent factor the model showed the minimum prediction error (Root Mean PRESS ≈ 0.77). The achieved mean cumulative Q^2 was 0.33, and the mean cumulative R^2 was 0.68, indicating that process parameters explain a considerable amount of the hardness variation.

Integrating VIP surface texture parameters improved the model moderately. With two factors the model showed a minimum prediction error, similar to the baseline model. The mean cumulative Q^2 value increased slightly to $Q^2 \approx 0.34$, while a cumulative $R^2 \approx 0.86$ was achieved. These results show that surface texture parameters still provide additional information for predicting hardness, enabling a moderate improvement of model robustness and accuracy compared to process parameters alone. The predicted versus actual value plot for a representative model run, including deviation bands of ±1.5% relative to the ideal line, is shown in Figure 8.

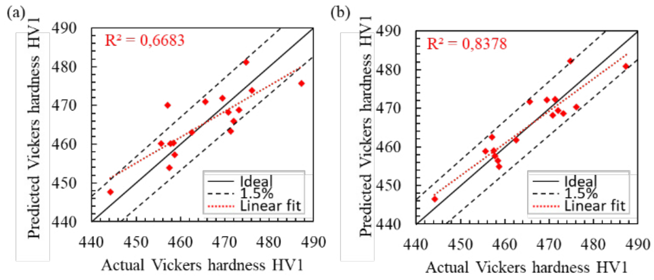

Fig. 8. Results of representative PLS regression models for hardness prediction: predicted versus actual values with deviation bands of ±1.5 % relative to the ideal line for (a) baseline model and (b) extended model.

5. Discussion

The PLS regression approach of this study, combining process parameters with VIP surface features, successfully improved density and hardness prediction. As shown in Figure 6, different VIPs were used for the two models. Due to the limited dataset size, overfitting cannot be entirely ruled out, although cross-validation and physically plausible VIP selection indicate robust trends.

For the density model, laser power exhibits the highest VIP value, thereby confirming the significant influence of this process parameter on component density [8, 21]. In addition, processing speed was selected as VIP, although ranked lower. Notably the line energy density was not selected as VIP.

In addition to the process parameters several surface texture parameters of the primary profile (P), roughness profile (R), and waviness profile (W) consistently show high relevance for density prediction. Among these, the highest peak-related descriptors (Rp, Wp, Pp) and the steepness-related values (Rku, Wku, Pku) ranked highest. In addition to the profile surface texture parameters, areal parameters were selected as important VIPs and similarly to the line related values, Sp and Sku are considered, although with lower VIP scores.

Amplitude-related descriptors, like the arithmetic mean of the largest absolute vertical distances between the maximum peak height and the maximum valley depth (Sz, Rz, Wz, Pz), the total height (Rt, Wt, Pt), the maximum height Ry and the reduced peak height Rpk capture the overall vertical extension of the surface topography and were also considered as VIP. Additional skewness-related values (Rsk, Wsk, Psk) appeared relevant. The aspect ratio of surface texture (Str) was also selected as VIP and is a measure of surface texture uniformity. This value may be associated with uneven material deposition and non-uniform melt pool wetting, favoring pore formation.

Process parameters like laser power and processing speed, strongly influence weld track formation and geometry as well as density [22, 23]. Balla et al. observed in DED an increase in track width and wetting angle, with increasing laser power, whereas increasing the scan speed led to a decrease in track height and wetting angle and a minor increase in width. Moreover, they concluded that weld track geometry strongly depends on size and shape of melt pool formed during deposition [22]. It can be deduced that track geometry capture significant information regarding process dynamics. Surface texture parameters related to steepness or skewness can be linked to track geometry and the overlapping of weld tracks, which influence melt pool solidification and local cooling rates, thereby affecting sub-surface porosity formation. Sharp peaks or high steepness values indicate uneven material deposition and potential lack of fusion, explaining why these descriptors dominate the density prediction model. The linkage to surface texture is physically motivated, but captures statistical correlations rather than explicit physical mechanisms.

Spatters reduce component quality as they can increase porosity and lead to irregular surface morphology [24]. According to Nagato et al. spatter data capture intermediate phenomena linking process parameters to performance values such as density and hardness [9]. Amplitude-related VIP mainly contain information from spatter. Consequently, they allow for consideration of spatter behavior, depending on the selected process parameters, within the model.

Considering those IFVs as VIPs takes the process dynamics, related to spatter formation and track geometry, into account within the density model. Taken together, the model improvement and respective VIP selection indicate that porosity is linked to fine-scale surface morphology, underlining the role of related IFV for density prediction. However, the purely data-driven approach does not explicitly model underlying physical mechanisms. Thus, the observed correlations should be interpreted as phenomenological, which limits direct generalizability. In addition, the present results are based on AISI 4140 steel, and alloy-dependent properties such as thermal conductivity, absorptivity, and solidification behavior may influence process characteristics like melt pool stability and spatter formation. Therefore, the identified relationships can only be transferred to other alloys after appropriate recalibration and validation.

It is noteworthy, that for the hardness model E_L, P_L and v were the top-ranked VIP, indicating a strong correlation to the Vickers hardness. This observation aligns with the findings reported by Yong et al., who noted that laser power and processing speed exert the most substantial influence on Vickers hardness. Specifically, an increase in laser power led to a reduction in hardness, while an enhancement in process speed resulted in an increase in hardness [25]. However, some surface texture parameters exceeded the threshold of VIP > 1, thereby demonstrating an influence on the Vickers hardness.

In addition to the aspect ratio of surface texture (Str) and the steepness-related parameters (Rku, Wku, Pku), which were already selected as VIP for the density model, RSm, PSm and WSm, representing the mean width of the profile elements ranked above the VIP threshold.

Moreover, the Root Mean Square (RMS) slope for the roughness profile (RΔq, PΔq, WΔq) appeared relevant.

An examination of the surface texture parameters indicates a potential correlation with track overlap during deposition. A broader melt track, in conjunction with a constant hatch distance, corresponds to a reduced mean width of the profile elements (RSm, PSm, WSm). Increased track overlap in broader tracks is also expected to affect the steepness (Rku, Wku, Pku) and the RMS slope (RΔq, PΔq, WΔq) of the surface profile. Broader weld tracks and thus higher overlap reduce the local cooling rate, which leads to reduced hardness [26, 27].

Sv, referring to the maximum pit height was selected as the only amplitude related parameter. The relevance of Sv may be explained by its sensitivity to local defects or instabilities, such as pore formation, which also affect the hardness [28].

6. Conclusion and Outlook

This explorative study investigated the use of surface texture parameters as intermediate feature values for predicting density and hardness in HS DED-LB. The predictive quality of models relying solely on process parameters was limited for density, whereas hardness could already be explained to a reasonable extent. By incorporating surface texture parameters, the density model improved substantially, achieving a more robust predictive performance. Contrary, the hardness model benefited only moderately, indicating that surface texture plays a secondary role compared to process parameters.

Overall, the findings support the hypothesis that surface-based IFV can capture relevant process phenomena and aid parameter identification, but also underline that their explanatory power remains limited. The results indicate that models trained on data from only two-layer samples transfer well to bulk samples, demonstrating the efficiency of the approach. Surface texture parameters complement but do not replace process parameters in predictive models. Especially for hardness, upstream IFV such as temperature data from pyrometry are expected to improve correlations with the underlying process mechanisms and model stability. Moreover, height-dependent hardness variations should also be addressed in future studies using upstream IFVs.

Further improvement of the predictive approach is expected from combining different types of IFV, complementing surface parameters with in-situ sensor data. Systematically integrating complementary IFV can bring future work closer to efficiently identifying parameters in HS DED-LB, supporting productivity and sustainability in remanufacturing applications.

Acknowledgements

Funded by the German Research Foundation (DFG, German Research Foundation) - SFB-1574 – 471687386.

This research was partially conducted at the University of Tokyo. We gratefully acknowledge the support from Prof. Nagato's group.

References

[1] G. Lanza, B. Deml, S. Matthiesen, M. Martin, O. Brützel, and R. Hörsting, “The vision of the circular factory for the perpetual innovative product,” *at - Automatisierungstechnik*, vol. 72, no. 9, pp. 774–788, Sep. 2024, doi: 10.1515/auto-2024-0012.

[2] J. Bennett *et al.*, “Repairing Automotive Dies With Directed Energy Deposition: Industrial Application and Life Cycle Analysis,” *Journal of Manufacturing Science and Engineering*, vol. 141, no. 2, p. 021019, Feb. 2019, doi: 10.1115/1.4042078.

[3] T. Schopphoven, “Experimentelle und modelltheoretische Untersuchungen zum Extremen Hochgeschwindigkeits-Laserauftragschweißen,” Aachen, 2019.

[4] A. Bagherzadeh, E. Budak, E. Ozlu, and B. Koc, “Machining behavior of Inconel 718 in hybrid additive and subtractive manufacturing,” *CIRP Journal of Manufacturing Science and Technology*, vol. 46, pp. 178–190, Nov. 2023, doi: 10.1016/j.cirpj.2023.08.004.

[5] S. Greco, M. Schmidt, K. Klauer, B. Kirsch, and J. C. Aurich, “Hybrid manufacturing: influence of material properties during micro milling of different additively manufactured AISI 316L,” *Prod. Eng. Res. Devel.*, vol. 16, no. 6, pp. 797–809, Jan. 2022, doi: 10.1007/s11740-022-01139-6.

[6] A. Singh, S. Kapil, and M. Das, “A comprehensive review of the methods and mechanisms for powder feedstock handling in directed energy deposition,” *Additive Manufacturing*, vol. 35, p. 101388, Jan. 2020, doi: 10.1016/j.addma.2020.101388.

[7] S. Greco, M. Schmidt, B. Kirsch, and J. C. Aurich, “Anwendungszentrum für additive Fertigung/Center for Applied Additive Manufacturing – Influence of process parameters during high-speed laser direct energy deposition,” *wt*, vol. 111, no. 06, pp. 368–371, Jan. 2021, doi: 10.37544/1436-4980-2021-06-12.

[8] H. Wexel, P. Fischmann, J. Schubert, and F. Zanger, “High-Speed DED-LB: Analysis of Process Control Variables as Enabler for Remanufacturing of Unique Products,” *Procedia CIRP*, vol. 127, pp. 230–235, 2024, doi: 10.1016/j.procir.2024.07.040.

[9] K. Nagato, T. Ozawa, M. Neuenfeldt, F. Zanger, M. Zhao, and V. Schulze, “Enhancing the prediction quality of mechanical properties for powder bed fusion with laser beam by dynamic observation of flying particles,” *Materials & Design*, vol. 227, p. 111696, Mar. 2023, doi: 10.1016/j.matdes.2023.111696.

[10] K. Nagato, R. Okawara, H. Yoshizaki, M. Sairaiji, and M. Zhao, “One-shot acquisition of intermediate feature values for in-process parameter exploration in PBF-LB of ultrafine porous metallic structure,” *CIRP Annals*, vol. 73, no. 1, pp. 445–448, 2024, doi: 10.1016/j.cirp.2024.04.099.

[11] M. Schmidt, S. Greco, B. Kirsch, and J. C. Aurich, “Analysis of Material Properties of Additively Manufactured Workpieces Using High-Speed Laser DirectedEnergy Deposition,” in *Production at the Leading Edge of Technology*, B.-A. Behrens, A. Brosius, W.-G. Drossel, W. Hintze, S. Ihlenfeldt, and P. Nyhuis, Eds., in Lecture Notes in Production Engineering. , Cham: Springer International Publishing, 2022, pp. 357–365. doi: 10.1007/978-3-030-78424-9_40.

[12] J. Schaible, D. Hausch, T. Schopphoven, and C. Häfner, “Deposition strategies for generating cuboid volumes using extreme high-speed directed energy deposition,” *Journal of Laser Applications*, 042034 vols., no. 34, pp. 1–9, Jan. 2022, doi: 10.2351/7.0000770.

[13] F. M. Sciammarella and B. Salehi Najafabadi, “Processing Parameter DOE for 316L Using Directed Energy Deposition,” *JMMP*, vol. 2, no. 3, p. 61, Sep. 2018, doi: 10.3390/jmmp2030061.

[14] J. Platz, M. Schmidt, K. Gutzeit, B. Kirsch, and J. C. Aurich, “Additive Fertigung von 17-4 PH Edelstahl durch Hochgeschwindigkeits-Laserauftragschweißen,” *Zeitschrift für wissenschaftlichen Fabrikbetrieb*, vol. 117, pp. 456–460, Jan. 2022, doi: 10.3390/app9163316.

[15] J. Jung *et al.*, “Effect of line energy on microstructures and mechanical properties of Co-Cr-Mo alloy single-track fabricated by DED method,” *Journal of Alloys and Compounds*, vol. 946, p. 169381, Jun. 2023, doi: 10.1016/j.jallcom.2023.169381.

[16] C. Hauschopp *et al.*, “Process development and heat flow analysis for thin walls made of aluminum using extreme high-speed laser material deposition (EHLA3D),” *Journal of Laser Applications*, vol. 36, 042052 vols., no. 4, Jan. 2024, doi: 10.2351/7.0001608.

[17] L. M. Carrascal, I. Galván, and O. Gordo, “Partial least squares regression as an alternative to current regression methods used in ecology,” *Oikos*, vol. 118, no. 5, pp. 681–690, May 2009, doi: 10.1111/j.1600-0706.2008.16881.x.

[18] S. Kramer, H. Wexel, A. Purwitasari, M. Jarwitz, V. Schulze, and F. Zanger, “Impact of different pore types on the tensile and fatigue properties of AlSi10Mg parts produced by laser powder bed fusion,” *Prog Addit Manuf*, Aug. 2025, doi: 10.1007/s40964-025-01288-x.

[19] P. Hoier, D. K. Santhosh, E. Hryha, and P. Krajnik, “An investigation into the grindability of additively manufactured 42CrMo4 steel,” *CIRP Annals*, vol. 73, no. 1, pp. 257–260, 2024, doi: 10.1016/j.cirp.2024.04.039.

[20] K.-H. Choi, J.-R. Cho, and D.-S. Shim, “Effect of heat transfer in substrate on microstructure and tensile behavior of deposits built by directed energy deposition,” *Journal of Materials Research and Technology*, vol. 28, pp. 3911–3931, Jan. 2024, doi: 10.1016/j.jmrt.2023.12.234.

[21] Pei-Yi Lin, Fang-Cheng Shen, Kuo-Tsai Wu, Sheng-Jye Hwang, and Huei-Huang Lee, “Process optimization for directed energy deposition of SS316L components,” *The International Journal of Advanced Manufacturing Technology*, pp. 1387–1400, Jan. 2020.

[22] S. K. Balla, M. Manjaiah, N. Selvaraj, and S. Bontha, “Effect of Process Parameters on Track Geometry and Porosity in Laser Direct Energy Deposition of High Strength Aluminum Alloy,” in *Processing and Fabrication of Advanced Materials, Volume 2*, vol. 53, A. Kumar, T. S. Srivatsan, M. Ravi Sankar, N. Venkaiah, and S. Seetharamu, Eds., in Springer Proceedings in Materials, vol. 53. , Singapore: Springer Nature Singapore, 2024, pp. 221–231. doi: 10.1007/978-981-97-5963-7_15.

[23] J. Schaible, L. Sayk, T. Schopphoven, J. H. Schleifenbaum, and C. Häfner, “Development of a high-speed laser material deposition process for additive manufacturing,” *Journal of Laser Applications*, vol. 33, no. 012021, pp. 1–9, Jan. 2021, doi: 10.2351/7.0000320.

[24] A. Sikandar Iquebal, A. Yadav, B. Botcha, R. Krishna Gorthi, and S. Bukkapatnam, “Tracking and quantifying spatter characteristics in a laser directed energy deposition process using Kalman filter,” *Manufacturing Letters*, vol. 33, pp. 692–700, Sep. 2022, doi: 10.1016/j.mfglet.2022.07.086.

[25] Z. Yong *et al.*, “Parameter optimization of T800 coating fabricated by EHLA based on response surface methodology,” *Optics & Laser Technology*, vol. 158, p. 108837, Feb. 2023, doi: 10.1016/j.optlastec.2022.108837.

[26] D. Tanigawa *et al.*, “Effect of laser path overlap on surface roughness and hardness of layer in laser cladding,” *Science and Technology of Welding and Joining*, vol. 20, no. 7, pp. 601–606, Oct. 2015, doi: 10.1179/1362171815Y.0000000044.

[27] I. Mathoho and T. Sibisi, “The influence of hatch spacing on the metallurgical characteristics of 17–4 PH stainless steel processed by DED,” *Int J Adv Manuf Technol*, vol. 130, no. 9–10, pp. 4565–4574, Feb. 2024, doi: 10.1007/s00170-023-12748-5.

[28] N. D. Dejene, W. M. Tucho, and H. G. Lemu, “Effects of Scanning Strategies, Part Orientation, and Hatching Distance on the Porosity and Hardness of AlSi10Mg Parts Produced by Laser Powder Bed Fusion,” *JMMP*, vol. 9, no. 3, p. 78, Feb. 2025, doi: 10.3390/jmmp9030078.